

Fabrication of Suspended Stratified Plasmonic Waveguides

Peter A.C. Neathway¹, Hui Yuan¹, Isobel C. Bicket¹, Erik Dujardin², Gianluigi A. Botton^{1,3},

¹Department of Materials Science and Engineering, McMaster University
1280 Main St. W., Hamilton, Canada
neathwap@mcmaster.ca; yuanh9@mcmaster.ca; bicketic@mcmaster.ca

²Laboratoire Interdisciplinaire Carnot de Bourgogne (ICB),
CNRS UMR 6303, Université de Bourgogne,
9 avenue A. Savary, 21000 Dijon, France
erik.dujardin@cnrs.fr

³Diamond Light Source
Diamond House, Harwell Science and Innovation Campus, Fermi Ave, Didcot, United Kingdom
gbotton@mcmaster.ca
Conference Centre - University of Toronto, Toronto.ca

Abstract – Tailored design of plasmonic nanoantennas typically involves electron beam lithography and eventually results in monolithic structures over a transmission electron microscope grid window. This approach is suited to the rapid production of many such structures; however, it requires several time-consuming steps and careful control of several factors. Here, we present the fabrication of plasmonic waveguides using a combination of plasma focused-ion beam (PFIB) techniques and single-crystalline gold flakes with nanoscale thicknesses. We dropcasted said flakes onto a silicon substrate with an oxide layer, deposited protective layers to shield the gold from ion implantation, and then used standard FIB procedures to extract a cross-sectional lamella from the stack. This lamella was then attached to a FIB grid *via* a micromanipulator and milled to the desired dimensions. The resultant structure was suspended over vacuum like a cantilever, facilitating excitation and measurement of plasmonic properties through electron energy loss spectroscopy in a scanning transmission electron microscope in aloof trajectories. Our results unequivocally demonstrate the fabrication of a stratified waveguide with a nanoscale gold layer, and that this platform can produce strong plasmonic signals.

Keywords: nanofabrication; spectroscopy; plasmonics; PFIB

1. Introduction

Scanning transmission electron microscopy (STEM) enables the positioning of an electron beam near metallic nanostructures. Electrons passing quickly by an interface between a metal and dielectric can excite oscillations in the charge density confined to such an interface, known as surface plasmon polaritons (SPPs) [1]. The corresponding energy loss can be collected using electron energy loss spectroscopy (EELS) [2]. Raster scanning the beam position over a region enables mapping of the spatial and spectral distribution of the plasmonic modal features [3-7]. These SPPs are of interest to several fields, including optical circuit components, because SPPs can be confined to spatial regions in a metallic nanoparticle much smaller than the corresponding free-space wavelength [7-11]. SPPs have also been shown to preserve entanglement when excited by quantum light [12-19]. Fabrication of metallic nanostructures is often facilitated by electron beam lithography [20], and the sputtering process of metals, atop substrates that are nearly transparent to the relevant wavelengths. These steps can be time-consuming and leave the possibility for the substrate to interfere with the plasmon resonance and directly affect the results. Importantly, it also usually results in the production of a single-layered structure (though these techniques can laboriously be extended to multi-step lithography for multi-layered structures [21]).

Alternatively, plasma focused-ion beam (PFIB) instruments equipped with scanning electron microscopes (SEM), are often used to lift-out cross-sectional slices from specimens as thin lamella [22]. PFIB-based ion-implantation, which could affect the plasmonic response by influencing the electronic configuration of the outer surface, can be mitigated by the deposition of protective layers over the surface prior to the lift-out process. We fabricated a stratified plasmonic waveguide, suspended over vacuum *via* attachment to a FIB grid, and characterized the response of the structure to electron beam

excitation *via* STEM-EELS. The structure studied herein was fabricated by dropcasting previously synthesized single-crystalline gold flakes [23] onto a silicon substrate with a silicon oxide layer. Poly-(methyl-methacrylate) (950 PMMA) was then spin-coated onto the surface at 6000 rpm for 90 s and baked at 175°C for five minutes. A 50 nm layer of evaporated carbon was deposited over the PMMA to decrease the amount of undesired exposure to said layer. An 11 μm gold flake was located, and then additional carbon and tungsten were deposited within the PFIB over the flake. Tungsten deposition allows for more control in the milling rate. The lift-out was performed (see preparation in Fig. 1a), and the resulting lamellar structure (5.9 μm x 6.5 μm x 24.2 μm) was attached to a FIB grid. Excess material was milled to produce the desired structure geometry (Fig. 1b). The FIB grid was then mounted into a single-tilt holder for the Nion HERMES electron microscope at the Canadian Centre for Electron Microscopy and investigated using EELS.

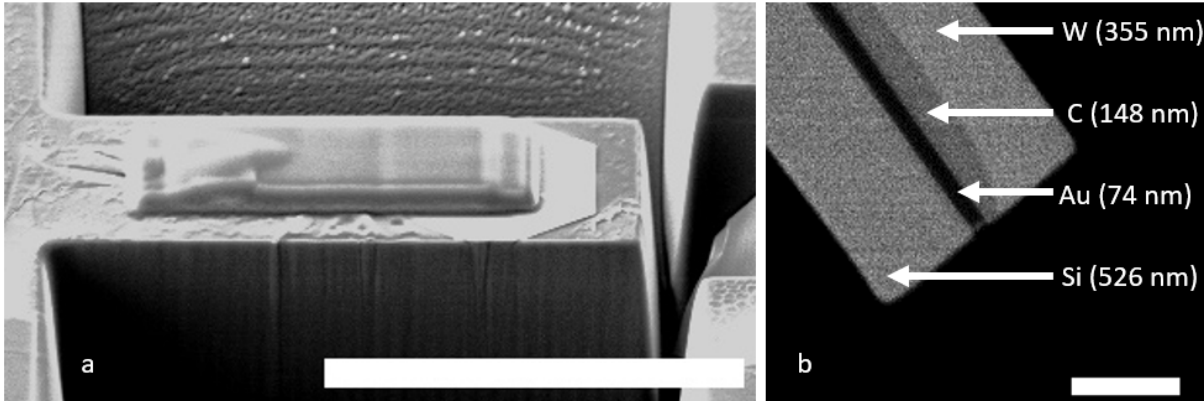


Fig. 1: a) SEM image of the selected region of our composite system in preparation for lift-out, scale bar is 20 μm . b) High-angle annular dark field (HAADF) image near the end of the completed structure, scale bar is 500 nm.

2. Results and Discussion

EELS maps displaying evidence of SPPs are shown in Fig. 2 for the first and second trajectories in Fig. 3. The distribution of the loss signals in these energy ranges is lobular, showing expected signs of evanescent fields extending into the surrounding vacuum. The lobes are indicative of standing waves formed by the SPPs [7,24] along the stratified structure. The normal and tilted EELS measurements indicate the distribution of the plasmonic modes in space. Point-spectra were collected near the end-facet and are shown in Fig. 3. There are at least seven distinct peaks, each successively indicating higher order standing wave patterns, and each of reasonably high quality factor. The comparison across the different tilts further suggests that the same modes are accessible in each of the analysed trajectories, and the delocalization indicates that the modes are not confined entirely to the gold layer.

Our PFIB-based approach to the fabrication of plasmonic structures can produce nearly freestanding waveguides supporting strong resonances. These have ultra-flat side facets, preferable to the typically slanted sidewalls of lithographically produced structures. Readily controlled thicknesses and sequences of layers means that stratification opens a broad design space for the creation of waveguides with chosen lateral dielectric environments. The way this structure is mounted onto the FIB grid enabled tilts of 45 degrees (and slightly higher; not shown), which is more than is normally possible with a standard TEM grid, perhaps enhancing the information which can be collected regarding the 3D photonic density of states around plasmonic structures, or other types of tomographic measurements [25-28]. This could also allow for optimization of inelastic delocalization or evanescent characteristics for coupling between multiple waveguides. Mounting the FIB grid along orthogonal orientations for two stage milling could enable three-dimensional (3D) design for even more control in the fabrication of plasmonic structures, in a consistent, repeatable, and adaptable framework.

3. Conclusion

In summary, we have developed a versatile methodology for the fabrication of suspended and stratified plasmonic waveguides supporting higher order resonances. This technique provides an important framework for control of the dielectric environment surrounding planar metallic components, and hence enables the direct tailoring of transverse fields extending away from the structure. Our approach has wide ranging applications for nanophotonics research.

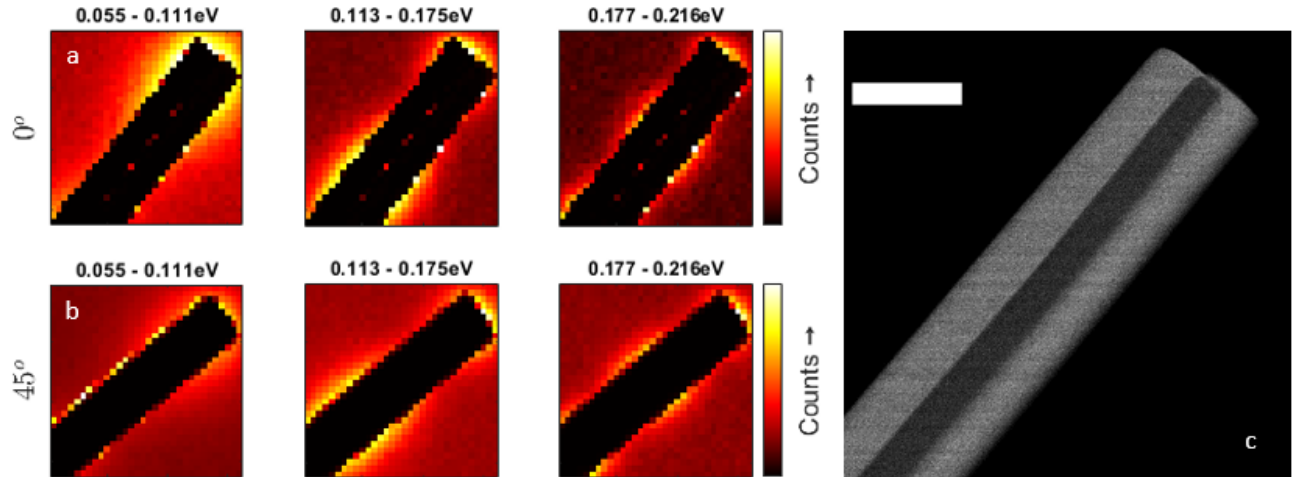


Fig. 2: Maps of the total intensity of EELS signal collected in the energy ranges listed above each image, around the stratified plasmonic waveguide, associated with a) 0° and b) 45° tilts. c) HAADF image collected for the same tilt as (b) with higher pixel depth, scale bar is $1 \mu\text{m}$.

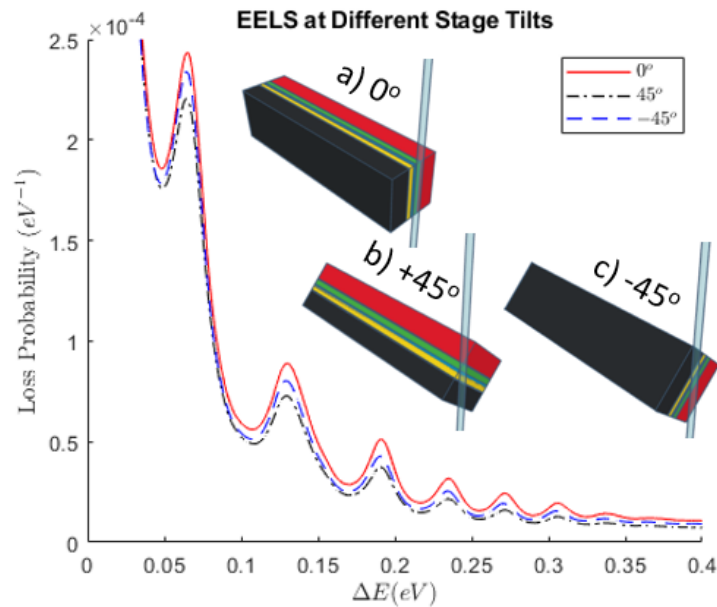


Fig. 3: EELS signals collected as high-count point spectra near the end-facet of the stratified structure at the three tilts.

Acknowledgements

The authors acknowledge the access to the PFIB and the Nion Hermes microscope at the Canadian Centre for Electron Microscopy, a facility supported by the Canada Foundation for Innovation, NSERC and McMaster University. This work is supported through a Discovery Grant to GAB.

References

- [1] J. M. Pitarke, V. M. Silkin, E. V. Chulkov, and P. M. Echenique, “Theory of surface plasmons and surface-plasmon polaritons,” *Reports on progress in physics* 70, 1, 2006.
- [2] R. F. Egerton, *Electron energy-loss spectroscopy in the electron microscope*. NY: Springer, 2011.
- [3] I. C. Bicket, E. P. Bellido, D. M. McRae, F. Lagugné-Labarhet, and G. A. Botton, “Hierarchical plasmon resonances in fractal structures,” *ACS Photonics* 7, 1246–1254, 2020.
- [4] E. P. Bellido, G. D. Bernasconi, D. Rossouw, J. Butet, O. J. Martin, and G. A. Botton, “Self-similarity of plasmon edge modes on koch fractal antennas,” *ACS Nano* 11, 11240–11249, 2017.
- [5] Y. Wu, G. Li, J. P. Camden, “Probing nanoparticle plasmons with electron energy loss spectroscopy,” *Chem. Rev.* 118, 2994–3031, 2017.
- [6] M. Kociak and O. Stéphan, “Mapping plasmons at the nanometer scale in an electron microscope,” *Chem. Soc. Rev.* 43, 3865–3883, 2014.
- [7] D. Rossouw and G. A. Botton, “Plasmonic response of bent silver nanowires for nanophotonic subwavelength waveguiding,” *Phys. Rev. Lett.* 110, 066801, 2013.
- [8] G. Volpe, G. Molina-Terriza, and R. Quidant, “Deterministic subwavelength control of light confinement in nanostructures,” *Phys. Rev. Lett.* 105, 216802, 2010.
- [9] D. Ballarini and S. De Liberato, “Polaritonics: from microcavities to sub-wavelength confinement,” *Nanophotonics* 8, 641–654, 2019.
- [10] S. A. Maier, “Plasmonics: Metal nanostructures for subwavelength photonic devices,” *IEEE J. Selected Topics Quantum Electronics* 12, 1214–1220, 2006.
- [11] R. F. Oulton, V. J. Sorger, D. A. Genov, D. F. P. Pile, and X. Zhang, “A hybrid plasmonic waveguide for subwavelength confinement and long-range propagation,” *Nat. Photonics* 2, 496–500, 2008.
- [12] H. Häsel, T. Moroder, and N. Lütkenhaus, “Testing quantum devices: Practical entanglement verification in bipartite optical systems,” *Phys. Rev. A* 77, 032303, 2008.
- [13] S. Fasel, M. Halder, N. Gisin, and H. Zbinden, “Quantum superposition and entanglement of mesoscopic plasmons,” *New J. Phys.* 8, 13, 2006.
- [14] E. Altewischer, M. P. Van Exter, and J. P. Woerdman, “Plasmon-assisted transmission of entangled photons,” *Nature* 418, 304–306, 2002.
- [15] G. Fujii, T. Segawa, S. Mori, N. Namekata, D. Fukuda, and S. Inoue, “Preservation of photon indistinguishability after transmission through surface-plasmon-polariton waveguide,” *Opt. Lett.* 37, 1535–1537, 2012.
- [16] S. Fasel, F. Robin, E. Moreno, D. Erni, N. Gisin, and H. Zbinden, “Energy-time entanglement preservation in plasmon-assisted light transmission,” *Phys. Rev. Lett.* 94, 110501, 2005.
- [17] J. S. Fakonas, H. Lee, Y. A. Kelaita, and H. A. Atwater, “Two-plasmon quantum interference,” *Nat. Photonics* 8, 317–320, 2014.
- [18] Y. J. Cai, M. Li, X. F. Ren, C. L. Zou, X. Xiong, H. L. Lei, B. H. Liu, G. P. Guo, and G. C. Guo, “High-visibility on-chip quantum interference of single surface plasmons,” *Phys. Rev. Appl.* 2, 014004, 2014.
- [19] M. C. Dheur, B. Vest, É. Devaux, A. Baron, J. P. Hugonin, J. J. Greffet, G. Messin, and F. Marquier, “Remote preparation of single-plasmon states,” *Phys. Rev. B* 96, 045432, 2017.
- [20] Y. Chen, “Nanofabrication by electron beam lithography and its applications: A review,” *Microelectron. Eng.* 135, 57–72, 2015.
- [21] I. C. Bicket, E. P. Bellido, S. Meuret, A. Polman, and G. A. Botton, “Correlative electron energy loss spectroscopy and cathodoluminescence spectroscopy on three-dimensional plasmonic split ring resonators,” *Microscopy* 67, i40–i51, 2018.
- [22] N. Antoniou, K. Rykaczewski, and M. D. Uchic, “In situ fib-sem characterization and manipulation methods,” *MRS Bull.* 39, 347–352, 2014.
- [23] Z. Guo, Y. Zhang, Y. DuanMu, L. Xu, S. Xie, and N. Gu, “Facile synthesis of micrometer-sized gold nanoplates through an aniline-assisted route in ethylene glycol solution,” *Colloids and Surfaces A: Physicochem. Eng. Aspects* 278, 33–38, 2006.

- [24] D. Rossouw, M. Couillard, J. Vickery, E. Kumacheva, and G. A. Botton, “Multipolar plasmonic resonances in silver nanowire antennas imaged with a subnanometer electron probe,” *Nano Lett.* 11, 1499–1504, 2011.
- [25] A. Hörl, A. Trügler, and U. Hohenester, “Full three-dimensional reconstruction of the dyadic green tensor from electron energy loss spectroscopy of plasmonic nanoparticles,” *ACS Photonics* 2, 1429–1435, 2015.
- [26] A. Hörl, A. Trügler, and U. Hohenester, “Tomography of particle plasmon fields from electron energy loss spectroscopy,” *Phys. Rev. Lett* 111, 076801, 2013.
- [27] A. Hörl, G. Haberfehlner, A. Trügler, F. P. Schmidt, U. Hohenester, and G. Kothleitner, “Tomographic imaging of the photonic environment of plasmonic nanoparticles,” *Nat. Comm.* 8, 37, 2017.
- [28] G. Haberfehlner, F. P. Schmidt, G. Schaffernak, A. Hörl, A. Trügler, A. Hohenau, F. Hofer, J. R. Krenn, U. Hohenester, and G. Kothleitner., “3d imaging of gap plasmons in vertically coupled nanoparticles by eels tomography,” *Nano Lett.* 17, 6773–6777, 2017.